Journal of Cell Science 113, 1033-1042 (2000)
Printed in Great Britain © The Company of Biologists Limited 2000
JCS0959

Evidence for the coincident initiation of homolog pairing and synapsis during the telomere-clustering (bouquet) stage of meiotic prophase

Hank W. Bass[1,2,*], Oscar Riera-Lizarazu[3,‡], Evgueni V. Ananiev[3], Stefano J. Bordoli[2], Howard W. Rines[3,4], Ronald L. Phillips[3], John W. Sedat[5], David A. Agard[5,6] and W. Zacheus Cande[1]

[1]Department of Molecular and Cell Biology, University of California, Berkeley, Berkeley, CA 94720, USA
[2]Department of Biological Science, Florida State University, Tallahassee, FL 32306-4370, USA
[3]Department of Agronomy and Plant Genetics, University of Minnesota, 411 Borlaug Hall, 1991 Buford Circle, St Paul, MN 55108-6026, USA
[4]US Department of Agriculture–Agricultural Research Service and [5]Department of Biochemistry and Biophysics, University of California, San Francisco, San Francisco, CA 94143, USA
[6]Howard Hughes Medical Institute, USA
*Author for correspondence (e-mail: bass@bio.fsu.edu)
‡Present address: Department of Crop and Soil Science, Oregon State University, Corvallis, OR 97331, USA
§Present address: Pioneer HiBred Intl, Johnston, Iowa, USA

Accepted 12 January; published on WWW 21 February 2000

SUMMARY

To improve knowledge of the prerequisites for meiotic chromosome segregation in higher eukaryotes, we analyzed the spatial distribution of a pair of homologs before and during early meiotic prophase. Three-dimensional images of fluorescence in situ hybridization (FISH) were used to localize a single pair of homologs in diploid nuclei of a chromosome-addition line of oat, oat-maize9b. The system provided a robust assay for pairing based on cytological colocalization of FISH signals. Using a triple labeling scheme for simultaneous imaging of chromatin, telomeres and the homolog pair, we determined the timing of pairing in relation to the onset of three sequential hallmarks of early meiotic prophase: chromatin condensation (the leptotene stage), meiotic telomere clustering (the bouquet stage) and the initiation of synapsis (the zygotene stage). We found that the two homologs were mostly unpaired up through middle leptotene, at which point their spherical cloud-like domains began to transform into elongated and stretched-out domains. At late leptotene, the homologs had completely reorganized into long extended fibers, and the beginning of the bouquet stage was conspicuously marked by the de novo clustering of telomeres at the nuclear periphery. The homologs paired and synapsed during the bouquet stage, consistent with the timing of pairing observed for several oat 5S rDNA loci. In summary, results from analysis of more than 100 intact nuclei lead us to conclude that pairing and synapsis of homologous chromosomes are largely coincident processes, ruling out a role for premeiotic pairing in this system. These findings suggest that the genome-wide remodeling of chromatin and telomere-mediated nuclear reorganization are prerequisite steps to the DNA sequence-based homology-search process in higher eukaryotes.

Key words: Meiosis, Chromosome, Telomere, Bouquet, Synapsis

INTRODUCTION

Meiosis is the specialized pair of cell divisions that normally results in the reduction of a cell's chromosome number by one half, giving rise to gametes or gamete-producing cells (John, 1990). A precise and balanced reduction of the nuclear genome to the haploid state via meiosis requires that the chromosomes in a diploid nucleus literally reorganize into the haploid number of homologous chromosome pairs. The precise two-by-two pairing of homologous chromosomes must be completed by meiotic prophase to ensure normal chromosome disjunction and segregation at the first meiotic division (for reviews, see John, 1990; Loidl, 1990; Kleckner, 1996; Roeder, 1997; Zickler and Kleckner, 1998).

Successful pairing and synapsis give rise to chromosome bivalents that can be observed by conventional microscopy during middle and late meiotic prophase. Although pairing and synapsis refer to similar and interrelated processes, important distinctions must be made when referring to analysis of meiotic chromosome behavior. The colocalization or touching of homologous chromosomes within the nucleus is generally referred to as *pairing*, sometimes called rough pairing, congressional pairing or alignment. *Synapsis* more specifically refers to coaxial connection of homologs, connected along their length by the synaptonemal complex, a conserved tripartite structure connecting meiotic chromosomes (von Wettstein et al., 1984). Synapsis is a hallmark of meiotic prophase and coincides with a specialized nuclear structure called the bouquet, in which telomeres are clustered on the nuclear envelope (Dernburg et al., 1995). The bouquet stage occurs in early meiotic prophase, is widely conserved in nature, and is therefore thought to play a central yet still unproven role in synapsis or crossover control

(Gelei, 1921; Hiraoka, 1952; Moens et al., 1989; Chikashige et al., 1994; Scherthan et al., 1996; Bass et al., 1997; Trelles-Sticken et al., 1999). The role of the bouquet in homolog pairing has been difficult to assess in light of the often conflicting data on the timing and nature of the homology-search process in plants, animals and fungi (Brown and Stack, 1968; Hawley and Arbel, 1993; Scherthan et al., 1994; Kleckner, 1996; Cook, 1997; Zickler and Kleckner, 1998; Franklin et al., 1999). A pressing question is whether homologs enter meiotic prophase already associated with each other or whether the search commences within meiotic prophase. The answer to this question has a direct bearing on the possible mechanisms of the search itself, namely, does the homology-search process function on interphase chromatin or condensed prophase fibers, and does the telomere clustering (bouquet stage) of meiotic prophase play a role in pairing or not?

To answer these and related questions, we have taken an approach based on three-dimensional imaging of fixed, intact meiotic nuclei from maize (Dawe et al., 1994; Bass et al., 1997). This approach allowed us to rule out premeiotic alignment of pairing at heterochromatic knob loci and to show that telomeres clustered de novo during meiotic prophase. Together these findings suggested that the homology search in maize did not commence until well within leptotene of meiotic prophase and that telomere rearrangements comprised an essential early step in pairing. Despite the certainty of staging and the accuracy of spatial measurements, the telomere study of Bass et al. (1997) lacked homolog pairing data, and the pairing study of Dawe et al. (1994) relied on detection of heterochromatic knob loci, leaving most of the homolog pairs unaccounted for.

In the present study, we set out specifically to determine whether the bouquet contributes to pairing by defining the timing of initial homolog contact relative to the timing of telomere clustering. We developed a novel triple labeling scheme for simultaneous imaging of chromatin, telomeres and a single pair of homologs. Here we have used this new system to inquire about the nature of the homology-search process and specifically the role of telomere behavior.

MATERIALS AND METHODS

Plant materials and fixation of reproductive organs

The maize-chromosome-9 disomic-addition line of oat used in this study was derived from second-generation disomic derivatives (2*n*=6X=42oat+2maize) of a partial oat×maize hybrid, ST633 (Riera-Lizarazu et al., 1996). ST633 is referred to throughout this paper as 'oat-maize9b' to distinguish it from the similar, but independently derived maize-chromosome-9 disomic-addition line ST505-5 (Ananiev et al., 1997, 1998). Oats were grown and meiotic stage florets harvested at the University of Minnesota as described by Riera-Lizarazu et al. (1996). Whole anthers were fixed by flotation in formaldehyde plus meiocyte Buffer A as described by Bass et al. (1997). Fixed anthers were stored in small airtight tubes in meiocyte Buffer A at 4°C until used. Anthers stored for more than 6 months were refixed for 15 minutes under the conditions described by Bass et al. (1997).

Maize DNA preparation and labeling and acrylamide FISH

Fluorescent oligonucleotide probes were used to stain telomeres with probe MTLF (5′-FITC[CCCTAAA]$_4$, see Bass et al., 1997) or to stain the 5S rDNA loci with probe ELMO-R (5′-ROX[GTCACCCATCCTAGTACTAC]-3′, Genset Oligos, La Jolla, CA, USA). The sequence chosen for the ELMO-R probe was based on the reverse complement of maize 5S rRNA from nucleotides 71-91 (Barciszewska et al., 1994). Oligonucleotide probes were used at a final concentration of 1-5 μg/ml hybridization buffer.

Total maize DNA was purified by CsCl centrifugation following extraction from inbred W23 immature ear shoots (Cande laboratory stock, UC Berkeley greenhouse grown 199293) or inbred KTF ear shoots or seedling leaves (Knobless Tama Flint, Bass stock, UC Berkeley greenhouse grown). For large-scale DNA preparations, 1-3 g tissue was ground to a powder in liquid N_2 with mortar and pestle, transferred to a 50-ml plug-seal polypropylene conical tube, and held on dry ice for 2 minutes. DNA was extracted by addition of 15 ml DNA-EB (7 M urea, 0.3 M NaCl, 50 mM Tris-HCl, pH 8, 20 mM EDTA-NaOH (pH 8), 1% sarkosine, 20 mM dithiothreitol, 1% polyvinylpyrolidone, 1% polyvinylpolypyrolidone), tissue resuspension, and sequential phase extraction with equal volumes of Tris-buffered phenol, 1:1 phenol:chloroform and chloroform. The resulting aqueous phase was filtered through miracloth (Calbiochem, La Jolla, CA, USA), and the DNA precipitated by addition of one volume 90% isopropanol plus 0.44 M ammonium acetate-acetic acid (pH 4.5). The DNA was centrifuged at 10,000 ***g*** for 20 minutes followed by a 70% ethanol rinse and brief vacuum drying and then redissolved in CsCl for standard isopycnic centrifugation.

For maize DNA probe labeling, the DNA preparations were digested with *Eco*RI, precipitated, redissolved in deionized H_2O, and direct-labeled with FluoroRed dUTP (RPN2122, Amersham) by means of random-primed labeling in 20 μl reactions as follows. Labeling reactions contained 12.520 μg/ml boiled and ice-cooled *Eco*RI-digested maize total DNA, 0.2 mM each of dATP, dCTP and dGTC, 0.05 mM TTP, 0.05 mM FluoroRed dUTP, 1× hexanucleotide mix (from 10× hexanucleotide mix, 1277 081, Boehringer Mannheim) and 500 U/ml Exonuclease-Free Klenow (10 U/μl stock, E70057Y, USB), and the reaction was allowed to proceed for 12-16 hours at 37°C. DNA labeling reactions were precipitated by addition of 0.1 volume of 3 M sodium acetate, 0.1 volume 2 mg/ml glycogen and 3 volumes ethanol, followed by incubation at –20°C for 1 hour, microcentrifugation for 15 minutes at 4°C, aspiration of supernatant, and drying of the precipitate for 30 seconds in a spin vacuum chamber. Samples were redissolved at approx. 100 μg input DNA/ml H_2O and diluted tenfold for hybridizations. Thus, a 30-μl probe mix would contain approx. 300 ng maize DNA probe. FISH was carried out on acrylamide-embedded meiocytes as detailed by Bass et al. (1997).

Three-dimensional microscopy and image processing

All images were recorded with an Olympus IMT-2 wide-field microscope and one of two oil-immersion lenses: 60× NA 1.4 PlanApo (Olympus) and 100× NA 1.4 PlanApo (Nikon) (Hiraoka et al., 1991). In both cases, the data were oversampled in the *X*, *Y* and *Z* dimensions with typical *XYZ* voxel dimensions of 0.11×0.11×0.3 μm^3 with the deconvolution light microscope workstation described elsewhere (Dernburg et al., 1996a,b). Initial data were collected by CCD imaging over large areas such as a portion of a column of synchronous meiocytes, followed by three-dimensional iterative deconvolution (Chen et al., 1995). The resulting large data sets were then cropped around individual whole nuclei prior to 3-D modeling and spatial analysis. The images presented were adjusted for brightness and contrast by linear scaling, and multiple-wavelength images were pseudocolored. Through-focus projections were made under the 'display maximum intensity' option, which was determined to provide the best view of structures in the projections.

Model building and spatial analysis of chromosome positions

Individual nuclei were modeled and spatial data were extracted and mathematically analyzed with the Priism software (IVE3.2 and IVE3.3, software versions developed at UC San Francisco, Agard and Sedat) programs FindPoints, EditPolygon, VolumeBuilder and Clouds (Chen et al., 1996). We used EditPolygon to trace the edges of the

nucleus (DAPI image) manually with a mouse, drawing circles on each optical section for a given nucleus. VolumeBuilder was used to connect the polygon series into a single 3-D object with a closed and continuous surface area from which the nuclear volume and distance data were determined. The FISH signals representing the space occupied by the maize-9 homologs (rhodamine images) were edge-traced and connected into 3-D objects in the same way. Polygon edges for KTF-probed samples were automatically generated either by use of FindPoints with a threshold of 6-8 or by manual generation for the W23-probed samples because of the bright knob signals. VolumeBuilder was used to calculate the volume and maximum distance across each object. For analysis of interhomolog distances, the Clouds program was designed to generate and analyze the population of straight line distances within and between the volumetric objects. To generate randomized and average distances that characterize the available spatial relationships between and within objects, the Clouds program spikes the 3-D objects with randomly placed points, then measures distances between those points (see Figs 5 and 6). So that the distribution of distances from different nuclei can be coplotted, the distances are normalized to the maximum distance across the nucleus. Spheres of different sizes have the same distribution of distances when the distances are normalized to their diameters (Hammersley, 1950). For nuclei in which the homologs were touching, interhomolog distances could not be properly determined and were therefore omitted from the measurement averages reported in Table 1 for interhomolog relationships.

RESULTS

In order to understand the role of telomere dynamics in meiosis, we have applied 3-D molecular cytology to formaldehyde-fixed pollen mother cells using a polyacrylamide-embedding technique that preserves the spatial organization of the nucleus (Bass et al., 1997). In this study we have exploited a maize-chromosome-addition line of oat for the purpose of optically isolating a single pair of maize homologs as they enter and progress through early meiotic prophase, a stage historically refractory to cytological analysis of individual chromosome behavior. The recently developed disomic maize-chromosome-addition line of oat, oat-maize9b, has a normal complement of oat chromosomes (*Avena sativa*, AACCDD genome, 2*n*=6X=42) plus a pair of maize chromosome9 homologs (Riera-Lizarazu et al., 1996; Ananiev et al., 1997). The resulting genotype (2*n*=42+2) allowed us to develop a FISH probe that could be used to paint and localize an entire pair of homologs within intact nuclei. The inclusion of a telomere-specific probe in all samples provided a temporal and spatial marker for the onset of synapsis, known to be initiated near the ends of chromosomes located in the bouquet in other ogranisms (Burnham et al., 1972; Moens et al., 1989; Dernburg et al., 1995; Zickler and Kleckner, 1998).

Oat 5S rDNA loci pair during the bouquet stage

We first wanted to establish the timing of pairing for the oat chromosomes in the oat-maize9b addition line. Throughout this paper we use the term ‘pairing’ to refer to spatial colocalization of homologs or homologous loci, although we recognize that this definition does not distinguish homology-dependent pairing from the coincidental pairing that may occur in any given nucleus. We monitored the pairing of endogenous oat loci using FISH probes specific for 5S rDNA genes. The 5S rDNA genes are located in gene clusters that provide ideal FISH targets. Because the maize 5S rDNA genes are located on maize chromosome 2 (not 9), we could attribute the 5S rDNA FISH signals from oat-maize9b nuclei to loci on oat chromosomes.

The 5S rDNA FISH signal consistently produced four very bright spots and 6-10 dim spots in interphase nuclei, consistent with the identification of six pairs of 5S loci in oat species (Linares et al., 1996). The four very bright spots (Fig. 1, pink arrows) always resolved into two bright double-dot spots by late pachytene (Fig. 1C,F) and were therefore used to monitor pairing at two different oat chromosomal loci shown in Fig. 1. Because these bright double spots represented homologous pairing, we scored nuclei as having zero, one or two double spots, as indicators of no, partial or complete pairing, respectively, for the two pairs of loci (Fig. 2). Nuclei were staged by chromatin morphology and telomere distribution as described by Bass et al. (1997) and as illustrated in the DAPI images of Fig. 1. Representative nuclei at leptotene (Fig. 1A), zygotene (Fig. 1B) and pachytene (Fig. 1C) show the difference in chromatin morphology and fiber appearance that is evident before, during and after telomere clustering, respectively. At leptotene (Fig. 1A,D), 5S rDNA loci were unpaired, and telomeres were not clustered (Fig. 1D). At zygotene, the telomere cluster is evident (white arrow, Fig. 6E), and the oat 5S rDNA loci in this example are still unpaired (Fig. 1E, pink arrows).

We plotted the pairing scores for nuclei and found that, in prebouquet nuclei (*n*=6 optical reconstructions), the oat 5S rDNA loci were all scored as 0 (no pairing, Fig. 2). The bouquet

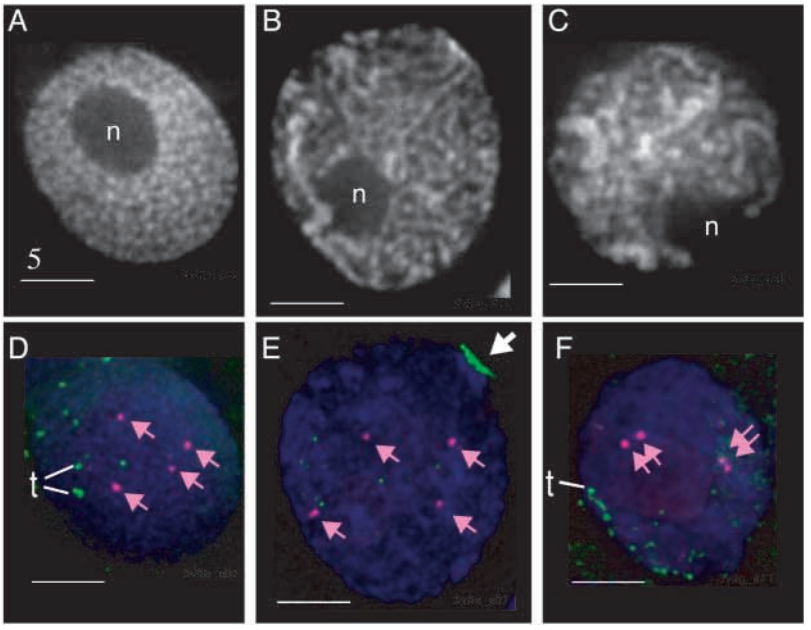

Fig. 1. Pairing kinetics of oat 5S rDNA signals. (A-C) DAPI images of 2-μm-deep medial projections of nuclei at leptotene (A), zygotene (B) and pachytene (C). The DAPI-free region indicates the position of the nucleolus (n). (D-F) Three-color overlay of whole-nucleus projections showing the positions of telomeres (t, green spots, and bouquet at white arrow in E) and 5S rDNA signals (pink spots and pink arrows). DAPI images in these projections are shown as dark blue. Scale bars, 5 μm.

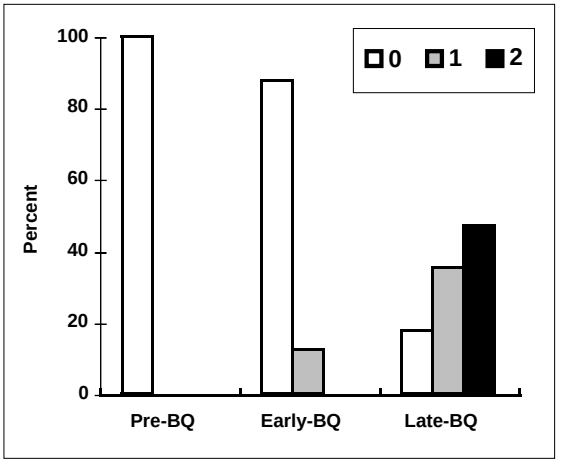

Fig. 2. Pairing configurations of oat 5S rDNA loci. The four brightest 5S rDNA FISH signals (see Fig. 1) represent two pairs of homologous loci. Each nucleus for the stages indicated was assigned a pairing status from one of three categories: '0' for none paired (separate spots), '1' for one paired (double dot), and two separate, or '2' for both paired (two double dots). The percentage of nuclei in each pairing category is plotted for prebouquet nuclei (Pre-BQ, premeiotic interphase through middle leptotene), early bouquet (Early-BQ, for late leptotene through middle zygotene), and late bouquet (Late-BQ for late zygotene).

stage spans all of zygotene and ranges from late leptotene to early pachytene (Bass et al., 1997). Thus early bouquet stages can be distinguished from late ones on the basis of the relative thickness of the chromosome fibers in the DAPI images. In columns of meiocytes at the early bouquet stage (n=8 nuclei), most of the 5S rDNA loci are unpaired (Fig. 2, EarlyBQ) and none of the nuclei showed pairing at both loci. At the late bouquet stage (n=17 nuclei), most nuclei show one or both of the bright 5S rDNA loci to be paired (Fig. 2, LateBQ). By pachytene (Fig. 1F), all nuclei showed two bright double spots (Fig. 1F). Similar double-dot pairing was observed at pachytene for the faint 5S rDNA loci (data not shown). Thus the endogenous oat 5S rDNA loci pair during the bouquet stage, providing a baseline for comparison with the pairing kinetics of the maize-9 homologs. Although the sample size was not large (n=31 nuclei scored), we did not find evidence for premeiotic colocalization of the two brightest pairs of oat 5S rDNA loci.

Genomic FISH probes from maize total DNA selectively 'paint' the maize-9 homologs

To visualize the maize chromosomes within the background of oat DNA, we developed FISH probes from maize total DNA preparations that were labeled with rhodamine-dUTP. The template DNA was prepared from either inbred line W23 or KTF (knobless Tama flint). We found that these probes gave surprisingly bright signals even without suppression of cross-hybridization with oat sequences. Although the target chromosomes were the same in each hybridization, the compositions of the probe DNA from W23 and KTF resulted in different patterns of painting, as shown in Fig. 3.

The FISH-painted maize-chromosome-9 images are shown below a drawing of maize-9 (Fig. 3A) to indicate the positions of a telomeric knob, K9S (terminal knob in 9S), and the centromere (Fig. 3A, Cent). Zygotene-stage nuclei stained with W23 FISH probes (Fig. 3B) or KTF FISH probes (Fig. 3C) resulted in a clear detection of the entire axial path of the maize-9 chromosome. The rhodamine images from 3D data stacks are displayed here as 2D projections (Fig. 3B,C, left side). The paths of the chromosomes were traced and computationally straightened (Fig. 3B,C, right side). The path lengths for the four chromosomes in these two nuclei were nearly identical, each measuring approximately 34 μm (Fig. 3B,C, right). The FISH signals that produced these images are believed to result from hybridization with the repetitive DNA of maize, which would be in relative molar excess in the probe compared with the unique or genic sequences. The remarkable lack of cross hybridization of these probes with oat chromosomes presumably reflects the divergence of repeat

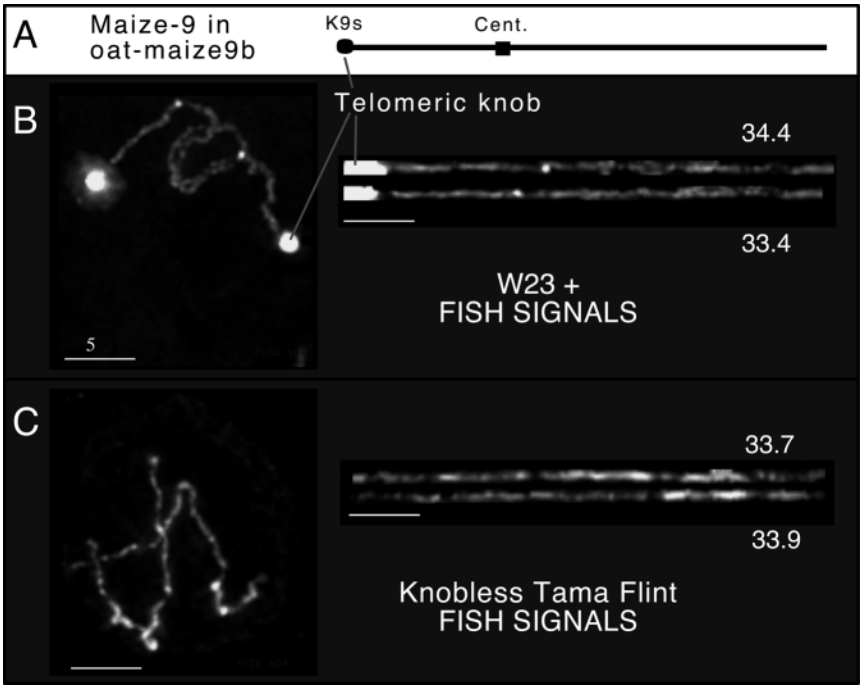

Fig. 3. Chromosome painting images of the maize-9 chromosome at meiotic prophase. (A) Chromosome 9 from maize karyotype shows the submetacentric position of the centromere (black square) and the location of the terminal knob on the short arm (K9s). (B) Rhodamine image (through-focus projection) of a single nucleus subjected to FISH with fluorescently labeled W23 maize DNA (see Materials and Methods). This nucleus is at the bouquet stage. The 3-D path of the chromosome was traced and computationally straightened (at right), showing the total path length in μm and indicating the bright signals attributed to the K9s knob sequences, in molar excess in the probe. (C) Same as B, but with the fluorescently labeled KTF maize DNA as a FISH probe (lacking knobs). Bars, 5 μm.

sequence composition between the evolutionarily divergent oat and maize genomes.

The W23 probe (Fig. 3B) resulted in a very bright signal at one end of the maize-9 chromosome. We believe the bright signal results from hybridization of knob repeat sequences in the probe mix to a knob sequence cluster, K9S, at the end of the short arm of maize-9. The knob sequences are expected to be at least 330 times more abundant in W23 than in KTF on the basis of copy-number-reconstruction Southern blots hybridized with a cloned knob DNA probe (H. W. Bass, data not shown). We did not determine which end of the KTF chromosomes corresponds to the K9S end, although a distinct pattern of FISH-dependent chromomeres is evident, especially when they are viewed as spinning stereo pairs (not shown). These data show that we have established robust chromosome-painting conditions for single-wavelength imaging of an entire chromosome inside the nucleus of morphologically preserved meiocytes.

Maize-9 homolog domains transform from clouds to extended fibers during leptotene

With a chromosome-painting protocol in place, we could study homolog positions and configurations independently of chromosome condensation status. The anthers of oat, like those of most higher plants, contain columns of synchronous meiocytes. The meiocytes used for the homolog pairing experiments were imaged in 3-D as groups of cells within columns of meiocytes. Each data set comprised three wavelength images per optical section (DAPI, FITC and rhodamine, see Materials and Methods). Data collected in this way allowed us to localize simultaneously the nucleus, the telomeres and the maize-9 homologs. Meiocytes were staged after imaging according to the appearance of the chromatin/fiber morphology as the primary criterion (DAPI images, e.g. Fig. 1) and the distribution of telomeres as a secondary criterion, leading to an unambiguous identification of nonbouquet nuclei as before or after zygotene as was described for maize (Bass et al., 1997). Here, synapsis is defined as the fusion of part or all of the maize-9 homologs into a single fiber. Although we did not have markers for the direct detection of the synaptonemal complex, the fusion of maize-9 fibers served as a good indicator of synapsis.

We first wanted to know about the organization of the maize-9 homologs as cells entered into meiotic prophase. Could we find evidence for premeiotic alignment, and were the chromosomes distributed throughout the nucleus as shown in Fig. 3, but in a more diffuse state? To our surprise we found that the maize-9 homologs in cells at premeiotic interphase occupied small compact domains as shown in Fig. 4. Telomeres (Fig. 4D, green dots) at premeiotic interphase were usually peripheral and loosely polarized but not tightly clustered in the bouquet configuration. Fig. 4A shows a projection of part of a column of premeiotic interphase cells (Fig. 4A, m), along with a row of nonmeiotic tapetal cells (Fig. 4, tp) across the upper left. The approximate direction of the column axis is indicted (yellow dashed lines, Fig. 4A-C). The chromosomes in the tapetal cells are also compact and cloud-like (Fig. 4A and more than 50 others examined and not shown). Stereo-pair projections of a representative nucleus at premeiotic interphase (Fig. 4D) show that the maize-9 homolog FISH signals can be spatially separate and that the homologs are not strung out across the nucleus as they are in nuclei later in meiotic prophase (Fig. 3).

At leptotene (Fig. 4B) the DNA shows pronounced condensation when viewed as gray-scale DAPI images, one optical section at a time (not shown, but see Fig. 1A for example). Telomere FISH signals were often at the nuclear periphery but still not tightly clustered in the bouquet configuration (Fig. 4E, green dots). Interestingly, the maize-9 homolog signals began to show a dramatic departure in shape from the compact cloud domains seen in interphase cells. At this stage, one or both maize-9 homologs appear to be partly elongated, reflecting an intermediate in the transformation from an interphase cloud-like structure to an extended chromosome fiber. The synchrony of meiocytes is revealed by the ‘cloud to fiber’ intermediate shape that appears for most of the maize-9 homologs in a single column (Fig. 4B). Thus the partly elongated homologs can be used to identify a narrow developmental time interval within leptotene (middle leptotene) that occurs after the first signs of chromatin condensation (early leptotene) but before the onset of telomere clustering (late leptotene).

During the bouquet stage, starting just before and ending just after zygotene, the maize-9 homologs were always found to be organized as long thin fibers (Figs 3, 4C,F). The trajectories of the homolog paths were highly variable. Even within and between nuclei in a synchronous column, the homologs were variable in position relative to each other and relative to the location of the bouquet (compare nuclei in Fig. 4C). In addition, the maize-9 homologs were variable with respect to which and how many of their four possible ends were located within the bouquet cluster. We observed nuclei with either zero, one, two, three or all four maize-9 telomeres in the bouquet cluster (see Fig. 4C). The most common of these were bouquet-stage nuclei with two or three maize-9 telomeres in the cluster. Unlike that in maize, the bouquet in oat did not contain all of the telomere FISH signals. In fact, only 70-90% of all telomere FISH signals were observed in the bouquet in any one nucleus. Therefore the observed fraction of maize-9 telomeres in the bouquet was similar to the overall fraction of oat telomere signals in the bouquet.

The stereo pair projection shown in Fig. 4F shows that synapsis has been initiated at the ends of the chromosome that are in the bouquet. This configuration also illustrates one of the inherent difficulties in making general statements about pairing progression from single site probes (see Discussion). An important finding from analysis of the bouquet stage nuclei was that, in some nuclei, homologs were still completely unpaired (e.g. Fig. 3C), requiring the homology-search machinery to function on condensed and extended chromosome fibers. At this stage, an alternative hypothesis remained that nuclei with completely separated homologs at the bouquet stage represented a small fraction of nuclei in which pairing of the maize-9 homolog had not been completed.

Although the maize-9 homologs showed remarkable variation within columns, the telomere distribution patterns did not. Thus, we think that the variation in the arrangements of the homologs was based not on a loss of synchrony in a given column but rather on some degree of randomness associated with the position of the chromosomes in early meiotic prophase.

Homologs at premeiotic interphase and early to middle leptotene are spatially separated

We next wanted to quantify the interhomolog distance relationships in order to determine when homologs first come

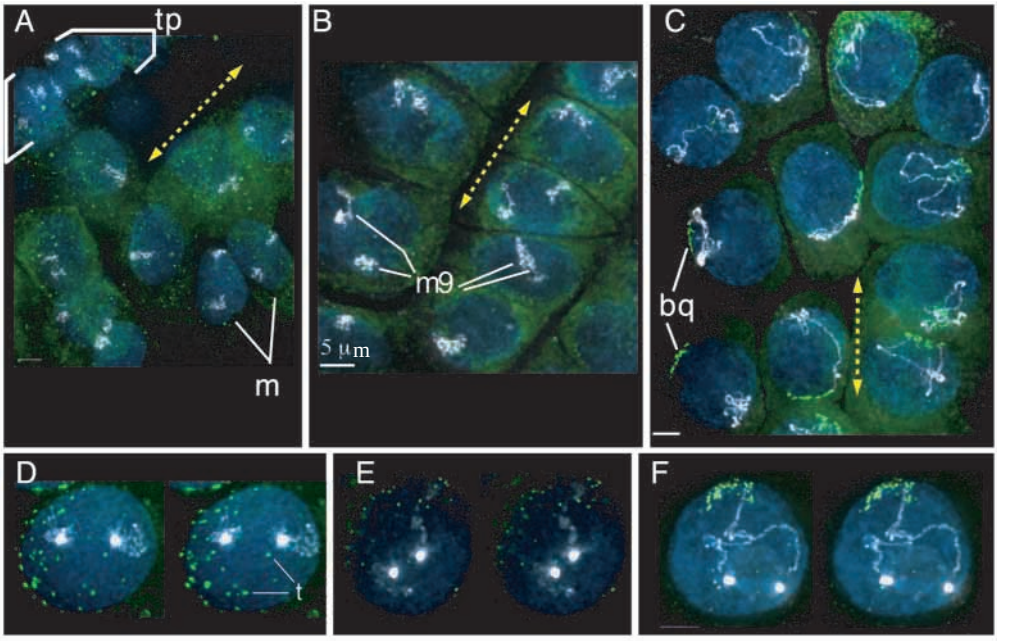

Fig. 4. Progressive reorganization of meiotic chromosomes. Columns of synchronous meiocytes (m) were subjected to FISH and 3-D deconvolution microscopy. Pseudocolored projections show DAPI in blue, FITC (telomeres) in green, and rhodamine (maize-9 homologs, labeled m9) in white (see Materials and Methods). The axis of the column is shown as a yellow dashed arrow. (A) Projection from a column of cells at premeiotic interphase. A row of tapetal cells is shown across the upper left (tp). The large meiocytes show the cloud-like domain organization of the maize-9 FISH signals. Two meiocytes with separated homologs are shown (m). (B) Projection from a column of cells at leptotene showing 'cloud-to-fiber' transition morphology of maize-9 homologs (m9). Telomere signals do not show up well in these deep projections, and they were primarily at the nuclear periphery, but not clustered. (C) Projection from a column of cells at the bouquet stage (early zygotene) showing conspicuous telomere clustering (bq) in each nucleus. Below each column is a stereo-pair projection of a single meiocyte from premeiotic interphase (D), middle leptotene (E) or zygotene (F). Telomeres (t, green dots) remain scattered even as the homolog begins to elongate at leptotene (E). (F) Synapsis has commenced at the end of the maize-9 that is in the telomere bouquet, whereas the other end (K9s end in this case) remains separate. Genomic FISH probes were made from KTF DNA (A-C) or W23 DNA (C-F). Bars, 5 µm.

into contact and how far apart they are at the onset of meiotic prophase. We built computerized models of the edges of the homologs' FISH signals and the edges of the nucleus, then used the 3-D spatial coordinates preserved in the models to extract real-space distance and volume information for the homologs. The methodology is illustrated for one nucleus in Fig. 5. A premeiotic interphase nucleus with separated homologs (two discontinuous FISH signal regions) is shown in Fig. 5A. Semiautomated region-finding programs (see Materials and Methods) were employed to define the edges of the maize-9 FISH signals (Fig. 5B, XS and enlarged inset) as shown for a single optical section. The large outer polygon (Fig. 5B, Nucl.) was modeled in the DAPI image (not shown) and represents the outer boundary of the nucleus. Reiteration of this process through the whole data stack results in a series of polygons that are connected to create closed-surface objects (see Materials and Methods).

The objects that correspond to the nucleus and chromosomes are then spiked with randomly placed points (Fig. 5C) to generate two populations of distances. The first contains the pair-wise distances between random points in the whole nucleus, which characterize the available space in the nucleus (see Materials and Methods) for comparison to the actual interhomolog distances. The second contains the pair-wise distances between points within the two homologs, which provide a comprehensive measure of the range of possible

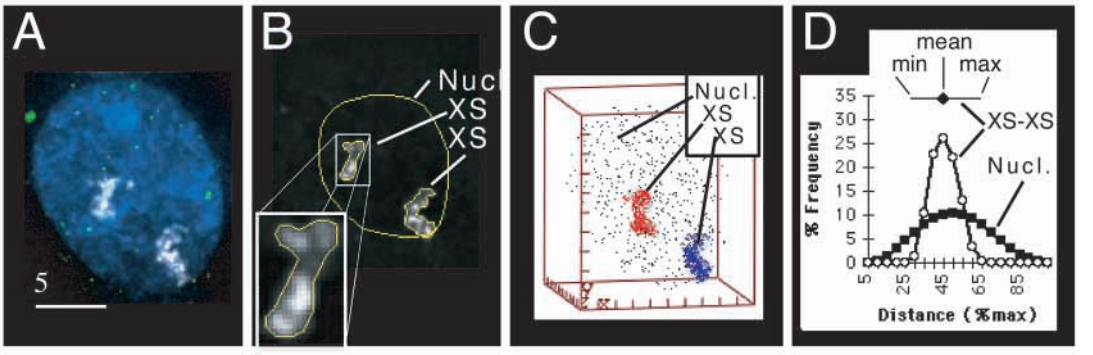

Fig. 5. 3-D modeling for analysis and plotting of interhomolog distances. (A) Three-color projection (as described in Fig. 4) of a cloud-staged premeiotic interphase nucleus. (B) Single optical section showing maize-9 FISH signals and edge tracings of the nuclear boundary (big yellow polygon, Nucl) and chromosomes (small polygons and zoomed inset, XS). (C) 3-D model of randomly placed points within the polygon-defined volumes (see Materials and Methods). Points are shown for the nuclear space (black, Nucl.) and the chromosome domain volumes (blue and red, XS). (D) The distribution of point-to-point distances that characterize the nucleus are normalized to the maximum distance across the nucleus and shown as a frequency histogram (Nucl.). A population of interhomolog distances is also normalized to the maximum distance across the nucleus and plotted in two ways, as a frequency histogram (XS-XS, open circles) and as a straight line (above curves) indicating the minimum (min, left end), maximum (max, right end) or mean interhomolog distance (mean, black diamond). Bar, 5 µm.

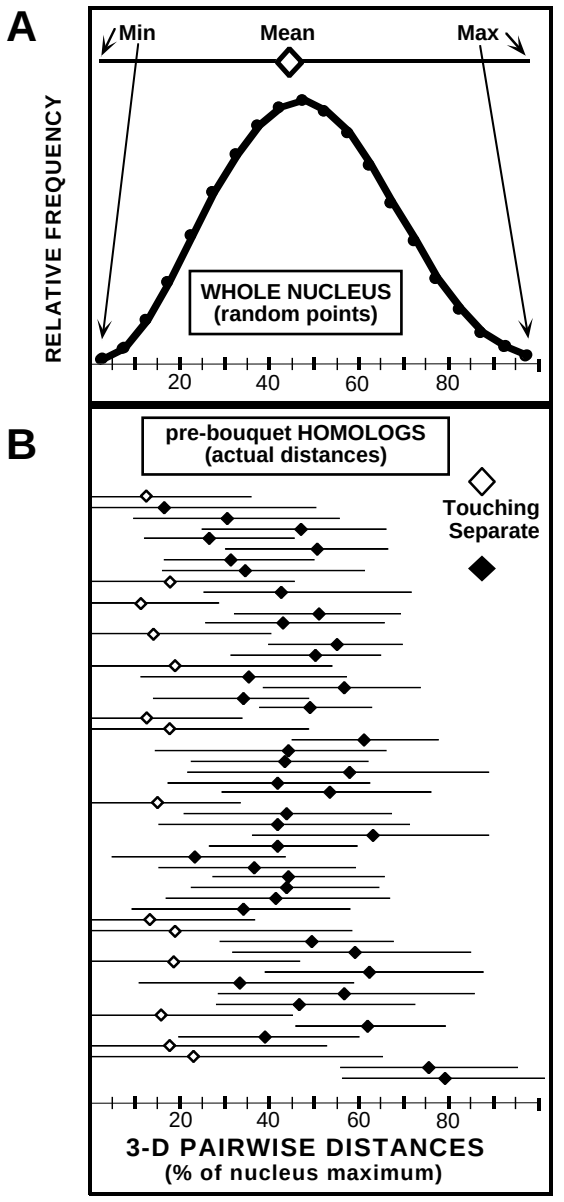

Fig. 6. Interhomolog distances in prebouquet nuclei. The normalized pairwise interhomolog distance distributions were determined and plotted as illustrated in Fig. 5 and described in Materials and Methods. (A) The distribution of distances is shown for a typical nucleus. The minimum distance (Min) is set to zero, and the maximum distance (Max) is 100. (B) The first 56 nuclei to be analyzed are plotted to illustrate the variation in interhomolog distances from nucleus to nucleus. Nuclei in which the homologs were touching are shown as open diamonds (see Materials and Methods), and those in which the homologs were separate are shown as solid diamonds.

interhomolog distances (minimum and maximum) as well as a mean. Because we could not identify specific subchromosomal loci within the maize-9 FISH signals, we decided to determine and report the population of interhomolog distances, both absolute and normalized to the nuclear maximum distance. The actual randomly placed points used for these measurements can be displayed as a 3-D model of the whole nucleus showing the nuclear points as black (Fig. 5C, Nucl.), and the homolog points as red or blue (Fig. 5C, XS). The distribution of distances in the nucleus can be plotted as a frequency histogram and, when normalized to the nucleus size, allows for comparisons among nuclei as previously described (Bass et al., 1997). The frequency histograms for the two populations of normalized distances described above are coplotted (Fig. 5D) and illustrate that the possible interhomolog distances (Fig. 5D, XS-XS) in this nucleus represent a subset of available nuclear distances (Fig. 5D, Nucl.). A simplified presentation of the interhomolog distance distribution is shown (Fig. 5D, straight line) as a one-dimensional line with an internal marker, revealing the minimum, maximum and mean interhomolog distance.

The methodology illustrated in Fig. 5 was used to measure distances for 74 nuclei as summarized in Table 1 and plotted in part in Fig. 6. We found that, on the whole, the maize-9 homologs at premeiotic interphase and up through middle leptotene occupied positions not dissimilar to those of randomly placed points in the nucleus. For nuclei in which the homolog signals were continuous (i.e. touching or paired) the minimum distance between homologs is zero (Fig. 6B, open diamonds) and the interhomolog distances calculated are the entire distribution of distances within single two-homolog space. Thus these distance populations are expected to be 'contaminated' with intrahomolog distances, making the minimum and mean pairwise distance values for 'touching' homologs artificially smaller to some degree. Even so, the mean interhomolog distance averaged over all nuclei is nearly the same as the average distance for the overall nuclear space.

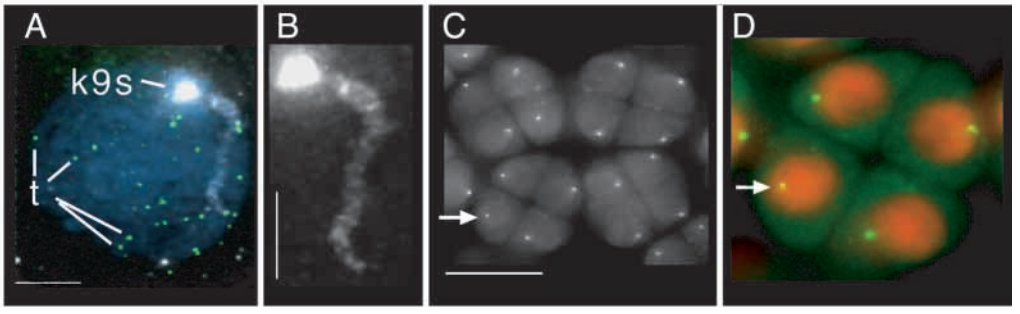

Fig. 7. Synapsis and segregation of maize-9. (A) A single pachytene nucleus is shown as a color projection as described in Fig. 4. The maize-9 FISH probe used in this case was W23 and therefore clearly stains the K9S knob sequences (k9s). At this stage, the bouquet has dispersed, as indicated by the scatter of telomere signals (t, green dots). (B) Inset zoom of the rhodamine image shows the completely synapsed maize-9 homolog along with substantial substructure and chromomeres. (C) Quartet nuclei were imaged with a 20× lens, and the bright dots (white arrow) in the rhodamine image are the K9S signals from W23-hybridized nuclei. (D) Close-up of a single quartet shows that the DAPI-stained nuclei (red) and the rhodamine FISH signals (green, arrow) colocalize. Bars, 5 μm.

Table 1. Nucleus and chromosome measurements from real-space 3-D models of intact nuclei

		Nucleus		Homologs				Separated interhomolog relationships[a]			
Stage[b]	*n*	Max. distance across (μm)	Vol. (μm^3)	Max. distance across (μm)[c]	Summed vol. (μm^3)	% Nucl. vol. (μm^3)[d]	% Separate[e]	Distance between centers (μm)[f]	Minimum distance (μm)	Mean pairwise distance (μm)[g]	Nucleus mean pairwise distance (μm)[h]
Cloud	49	18.4 (1.5)	1800 (430)	5.61 (1.4)	28.0 (10.9)	1.57 (0.55)	73	8.19 (2.3)	5.00 (2.3)	8.19 (2.4)	7.94 (0.53)
Cloud-to-fiber	25	17.8 (1.2)	1510 (170)	6.74 (1.9)	25.2 (7.2)	1.7 (0.5)	88	7.37 (2.2)	3.95 (1.5)	8.05 (1.8)	7.61 (0.3)
Fiber	41	21.8 (1.5)	3280 (470)	n.d.	n.d.	n.d.	5	n.d.	n.d.	n.d.	n.d.

Values are means (± s.d.); measurements are based on 3-D models built from DAPI images (nucleus) and rhodamine FISH images (maize-9 homologs). n.d., not determined.

[a]Measurements limited to nuclei with separated maize-9 homologs; *n*=36 (Cloud stage) and *n*=22 (Cloud-to-fiber stage).

[b]Data are pooled, according to maize-9 homolog morphology, into three sequential developmental stages with the following attributes. (1) Cloud stage: both homologs are organized as compact domains; premeiotic interphase and early leptotene; no bouquet. (2) Cloud-to-fiber transition stage: one or both homologs are partially elongated; middle leptotene; no bouquet. (3) Fiber stage: both homologs are organized as discrete thin fibers, late leptotene and zygotene, bouquet always present; variable degrees of synapsis.

[c]Measurements limited to nuclei with separated maize-9 homologs; *n*=72 homologs (Cloud) and *n*=44 (Cloud-to-fiber) homolog domains (2 per nucleus).

[d]Average of (sum of chromosome domain volumes/nuclear volume of same nucleus)×100.

[e]Percentage of nuclei in which maize-9 FISH signal regions were separated as two discontinuous domains.

[f]Distance between centers of space (pixel intensity-independent) calculated from spatial models of homolog domains.

[g]Mean 3-D pairwise distance between randomly positioned points within homolog volumes; *n*=10,000 interhomolog distances per nucleus (see Materials and Methods and Figs 5 and 6).

[h]Mean 3-D pairwise distance between randomly positioned points within whole nucleus; *n*=499500 distances per nucleus.

Even as homologs began to elongate in middle leptotene, 88% of nuclei showed separate homologs (Table 1). Furthermore, in several cases, homologs were scored as ‘paired’ or touching even though the FISH signals appeared as two equal-sized domains connected by only a few pixels. Therefore, the percentage of nuclei with meaningful pairing may be even less than suggested by Table 1. These data clearly demonstrate that the majority of homologs enter meiotic prophase separated by large distances, in contrast to prior reports of premeiotic alignment in other grasses (Maguire, 1983; Aragón-Alcaide et al., 1997; Schwarzacher, 1997; Martínez-Pérez et al., 1999).

Maize-9 homologs synapse and segregate

So as to interpret properly the distance and timing data described above, we wished to confirm that the maize-9 homologs were successfully passing through meiosis, as predicted from the ability to propagate the oat-maize9b line sexually (Riera-Lizarazu et al., 1996). In particular, was the seemingly high incidence of separate homologs at leptotene and zygotene correlated with a failure of the maize-9 homologs to synapse and disjoin? If so, we would be able to observe such failures at pachytene or in nuclei at the second meiotic telophase. Pachytene nuclei are recognized by the thick fibers in the DAPI images and by the partial or complete dispersal of the telomere bouquet. A projection of a representative pachytene nucleus is shown in Fig. 7A along with the gray-scale rhodamine image close-up (Fig. 7B). In 13 pachytene cells subjected to 3-D imaging, and in at least 30 cells that were inspected but not photographed, the maize-9 FISH signals stained single, synapsed thick chromosome fibers, measuring 20 μm in length and having some substructure and chromomeres. Thus synapsis appeared to go to completion.

Cells that have just completed meiosis II are always found together as a quartet, in which segregation can be directly observed. Individual nuclei from quartet-stage cells were scored for the presence of zero, one, two, three or four maize-9 FISH signals. In 100% of the 120 nuclei examined, we found only one maize-9 per nucleus (Fig. 7C,D). Taken together with the pachytene data, this result showed that the maize-9 homologs in the oat-maize9b lines are capable of proper synapsis and disjunction. Thus, the unpaired leptotene homologs did not indicate pairing failure. On the contrary, these results indicate that condensed, spatially separated chromosomes can find each other and that the homology search may function during and not before meiotic prophase.

DISCUSSION

Our primary aim was to determine the timing of homologous chromosome pairing (rough pairing or initial contact), which we found to coincide with the initiation of telomere clustering in late leptotene. Our findings and interpretations are strengthened by the clarity with which an entire homolog pair can be visualized and placed in a precise temporal sequence when chromatin morphology and telomere distribution are used as staging criteria. We also provide yet another cytological staging marker, the ‘cloud-to-fiber’ transition morphology of homologs at mid-leptotene, after the onset of meiotic prophase and just prior to telomere clustering.

We rule out the possibility that the maize-9 homolog pair introduced into the oat genome does not undergo normal pairing and synapsis on the following grounds. First, the timing of homolog encounter for maize-9 is consistent with that of the endogenous oat 5S rDNA sequences. Second, Dawe et al. (1994) measured the changes in spatial arrangement of knobs using 3-D imaging of DAPI-stained maize meiocytes. One of the knobs in that study was in fact K9S (see Fig. 3A), which was found to be unpaired until prezygotene, at which point the two K9S loci began to come together at the nuclear periphery. Thus the pairing kinetics of the 9S telomeres are the same in maize as in oat-maize9b. Third, the presence of the terminal knob in oat-maize9b indicates that at least the short arm of maize-9 is stable and not subject to terminal deletions. In fact,

13 of 13 maize-9-specific DNA markers spanning the chromosome were positive for DNA gel blot detection, consistent with the presence of an intact maize-9 chromosome in the addition line (O. Riera-Lizarazu, data not shown). Finally, the 100% efficiency of maize-9 segregation indicates proper pairing and disjunction. We therefore believe that the maize-9 chromosome is basically 'normal' and provides us with a reliable tool for study of chromosome behavior and nuclear architecture.

Implications for the mechanism of homology search

In discussing the mechanism(s) involved, we suggest that the homology search should be defined not only by the molecular DNA-DNA interactions (Kleckner, 1996) but also by the higher-order chromatin structure, chromosome packaging and nuclear organization that enable the homology search to produce stable interactions for synapsis between homologs. In this regard, the first steps of the homology search would be the obligatory genome-wide remodeling of chromosomes into condensed, extended fibers and the telomere-mediated reorganization of the entire nucleus so as to increase greatly the likelihood of homolog encounter.

A significant finding of this study is that, in 88% of the mid-leptotene-stage nuclei, maize-9 homologs were spatially separated, even though chromosome condensation and fiber formation were underway. The timing of pairing and lack of premeiotic pairing observed here is consistent with other 3-D studies of chromosomal pairing in human and maize (Dawe et al., 1994; Scherthan et al., 1998). In addition, Franklin et al. (1999) found that the recombination protein Rad51, thought to be directly involved in the homology search, forms discrete nuclear foci after the leptotene stage in maize meiocytes. Collectively, these studies identify the leptotene-to-zygotene transition as the start of both pairing and synapsis.

In contrast, Schwarzacher (1997) found that pairing in wheat involved a premeiotic 'cognition' whereby homologs interacted at premeiotic interphase, possibly mediated by the centromeres. Similarly, Aragón-Alcaide et al. (1997) analyzed the behavior of a pair of homologous barley chromosomes substituted into a polyploid wheat. In that study, homolog associations were observed in meiocyte and tapetum nuclei from anthers harvested prior to the onset of meiotic prophase. Even more recently, Martínez-Pérez et al. (1999) described evidence of premeiotic homolog interactions in wheat lines with chromosome additions or substitutions. The timing and nature of homolog pairing described for wheat is significantly different from our observations with the oat-maize9 material. In particular, we did not find evidence for separation of sister chromatids at the bouquet stage (note fibers of Fig. 3C). These differences may reflect species-specific differences in timing or mechanism of meiotic chromosome pairing between wheat and oat or maize. Premeiotic alignment in wheat may reflect an additional requirement to sort out the three related genomes of that species.

Our data provide a clear demonstration that, in most nuclei, the first homolog-to-homolog encounter occurs between chromosomes that are condensed or condensing and transforming into extended fibers. Thus, the homology search may operate most efficiently on condensed chromosome fibers whose termini are arranged in parallel by the bouquet. For example, extended fiber attachment to the nuclear envelope may allow an excess of subterminal homolog-to-homolog contacts that is collectively strong enough to withstand the telomere-based large-scale movements such as the nuclear movements observed in *Schizosacharomyces pombe* during the horse-tail (bouquet) stage of meiosis (Chikashige et al., 1994; Ding et al., 1998). In this scenario, one function of the bouquet and associated telomere motilities could be to destabilize heterologous interactions through physical movement of whole chromosome arms. Consistent with this idea, Lukaszewski (1997) demonstrated that asymmetric isochromosomes failed to undergo chiasmate pairing in wheat. In that study, heterozygosity for small terminal deletions had remarkable negative impact on chiasmate pairing, despite the presence of extensive, colinear homology in other regions of the isochromosomes (Lukaszewski, 1997). With respect to the bouquet structure, where chromosomes are polarized by end-on attachments to the nuclear envelope, such heterozygosity would produce chromosome misalignment of the terminal-most segment of the chromosome. Therefore, the bouquet structure may promote homolog encounter as part of the homology search, while also promoting synapsis by parallel alignment of chromosome ends, as proposed by Scherthan et al. (1998).

How do the telomeres move to the nuclear envelope at leptotene?

The dynamic transformation from cloud to fiber clearly involves chromosome movement within the nucleus and the clustering of telomeres on the nuclear envelope. Yet what is the mechanical force underlying these movements? One possibility is that the telomere-specific movements pull or string out the chromosomes by some type of intranuclear molecular motor. Alternatively, the formation of the axial element (or lateral element) of the meiotic chromosome could result in chromosome relocation, especially if the axial element were semirigid. If the leptotene fiber is twice the length of the nucleus (Fig. 3, Table 1) and its formation causes some degree of straightening out, then it may follow that initial formation of the extended fiber will drive the chromosome and its ends into the nuclear envelope. In this case, the entire nuclear envelope may be capable of capturing telomeres at late leptotene, followed by clustering once attached. Whatever the mechanism, the binding of telomeres all over the nuclear envelope followed by clustering is a well-documented sequence of events (Gelei, 1921; Scherthan et al., 1996).

Implications for interpreting prior pairing studies

The cloud-shaped domain organization found for premeiotic interphase and early leptotene nuclei has important implications for interpretation of pairing studies that use site-specific markers or probes to monitor pairing (Weiner and Kleckner, 1994; Dawe et al., 1994). At premeiotic interphase, a single locus roughly reports the position of an entire homolog because the homologs are organized as compact clouds (see Table 1, Figs 4A, 5A), but by mid-leptotene and into the bouquet stage, the same site-specific marker no longer reveals the general position of the homolog on which it resides. Consider for example the different interhomolog distances that would be measured for different sites along the maize-9 homolog in a bouquet-stage nucleus such as the one shown in Fig. 4F. Our results suggest that the utility of site-specific

probes as indicators of homolog positions varies with stage and in particular may underestimate pairing interactions during the bouquet stage.

In conclusion, we provided compelling cytological evidence that homologous chromosomes pair and synapse during the telomere bouquet stage, suggestive of a role for telomeres in the homology search process. With regard to the overall timing of meiotic prophase events, our findings with the oat-maize9b are similar to those of Scherthan et al. (1998) with human spermatocytes. Thus, the telomere-mediated reorganization of the early meiotic prophase nucleus may be a widely conserved first step in the homology search process of higher eukaryotes.

We thank H. Scherthan for helpful discussion of unpublished results during the early stages of this work, Diana D. Hughes for development of Priism software and the Clouds program, and A. Franklin and L. Harper for helpful comments on the manuscript. H.W.B. was supported as a D.O.E. postdoctoral fellow of the Life Sciences Research Foundation. S.J.B. was supported by a J. R. Fisher Fellowship from the American Cancer Society, Florida Division. This work was also supported by National Institutes of Health grants to W.Z.C. (R01-GM-48547) and to J.W.S. (R01-GM-25101-16). D.A.A. is an investigator of the Howard Hughes Medical Institute.

REFERENCES

Ananiev, E.V., Riera-Lizarazu, O., Rines, H. W. and Phillips, R. L. (1997). Oat-maize chromosome addition lines: a new system for mapping the maize genome. *Proc. Natl. Acad. Sci. USA* **94**, 3524-3529.

Ananiev, E. V., Phillips, R. L. and Rines, H. W. (1998). Complex structure of knob DNA on maize chromosome 9. Retrotransposon invasion into heterochromatin. *Genetics* **149**, 2025-2037.

Aragón-Alcaide, L., Reader, S., Beven, A., Shaw, P., Miller, T. and Moore, G. (1997). Association of homologous chromosomes during floral development. *Curr. Biol.* **7**, 905-908.

Barciszewska, M. Z., Erdmann, V. A. and Barciszewski, J. (1994). A new model for the tertiary structure of 5S ribonucleic acid in plants. *Plant Mol. Biol. Rep.* **21**, 116-131.

Bass, H. W., Marshall, W. F., Sedat, J. W., Agard, D. A. and Cande, W. Z. (1997). Telomeres cluster de novo before the initiation of synapsis: a three-dimensional spatial analysis of telomere positions before and during meiotic prophase. *J. Cell Biol.* **137**, 5-18.

Brown, W. V. and Stack, S. M. (1968). Somatic pairing as a regular preliminary to meiosis. *Bull. Torr. Bot. Club* **95**, 369-378.

Burnham, C. R., Stout, J. T., Weinheimer, W. H., Knowles, R. V. and Phillips, R. L. (1972). Chromosome pairing in maize. *Genetics* **71**, 111-125.

Chen, H., Swedlow, J. R., Grote, M. A., Sedat, J. W. and Agard, D. A. (1995). The collection, processing, and display of digital three-dimensional images of biological specimens. In *Handbook of Biological Confocal Microscopy* (ed. J. B. Pawley), pp. 197-210. Plenum Press, New York.

Chen, H., Hughes, D. D., Chan, T.-A., Sedat, J. W. and Agard, D. A. (1996). IVE (Image Visualization Environment): a software platform for all three-dimensional microscopy applications. *J. Struct. Biol.* **116**, 56-60.

Chikashige, Y., Ding, D.-Q., Funabiki, H., Haraguchi, T., Mashiko, S., Yanagida, M. and Hiraoka, Y. (1994). Telomere-led premeiotic chromosome movement in fission yeast. *Science* **264**, 270-273.

Cook, P. R. (1997). The transcriptional basis of chromosome pairing. *J. Cell Sci.* **110**, 1033-1040.

Dawe, R. K., Sedat, J. W., Agard, D. A. and Cande, W. Z. (1994). Meiotic chromosome pairing in maize is associated with a novel chromatin organization. *Cell* **76**, 901-912.

Dernburg, A. F., Sedat, J. W., Cande, W. Z. and Bass, H. W. (1995). Cytology of telomeres. In *Telomeres* (ed. E. H. Blackburn and C. W. Greider), pp. 295-338. Cold Spring Harbor Laboratories Press, Cold Spring Harbor, NY.

Dernburg, A. F., Broman, K. W., Fung, J. C., Marshall, W. F., Philips, J., Agard, D. A. and Sedat, J. W. (1996a). Perturbation of nuclear architecture by long-distance chromosome interactions. *Cell* **85**, 745-759.

Dernburg, A. F., Sedat, J. W. and Hawley, R. S. (1996b). Direct evidence of a role for heterochromatin in meiotic chromosome segregation. *Cell* **86**, 135-146.

Ding, D.-Q., Chikashige, Y., Haraguchi, T. and Hiraoka, Y. (1998). Oscillatory nuclear movement in fission yeast meiotic prophase is driven by astral microtubules, as revealed by continuous observation of chomosomes and microtubules in living cells. *J. Cell Sci.* **111**, 701-712.

Franklin, A. E., McElver, J., Sunjevaric, I., Rothstein, R., Bowen, B. and Cande, W. Z. (1999). Three-dimensional microscopy of the rad51 recombination protein during meiotic prophase. *Plant Cell* **11**, 809-824.

Gelei, J. (1921). Weitere Studien über die Oogenese des *Dendrocoelum lacteum*. II. Die Längskonjugation der Chromosomen. *Archiv für Zellforschung* **16**, 88-169, pls. 6-11.

Hammersley, J. M. (1950). The distribution of distances in a hypersphere. *Ann. Math. Stat.* **21**, 447-452.

Hawley, R. S. and Arbel, T. (1993). Yeast genetics and the fall of the classical view of meiosis. *Cell* **72**, 301-303.

Hiraoka, T. (1952). Observational and experimental studies of meiosis with special reference to the bouquet stage. XIV. Some considerations on a probable mechanism of the bouquet formation. *Cytologia* **17**, 292-299.

Hiraoka, Y., Swedlow, J. R., Paddy, M. R., Agard, D. A. and Sedat, J. W. (1991). Three-dimensional multiple wavelength fluorescence microscopy for the structural analysis of biological phenomena. *Semin. Cell Biol.* **2**, 153-165.

John, B. (ed.) (1990). Meiosis. *Developmental and Cell Biology Series* **22**. Cambridge University Press, New York. 396 pp.

Kleckner, N. (1996). Meiosis, how could it work? *Proc. Natl. Acad. Sci. USA* **93**, 8167-8174.

Linares, C., Gonzalez, J., Ferrer, E. and Fominaya, A. (1996). The use of double fluorescence in situ hybridization to physically map the positions of 5S rDNA genes in relation to the chromosomal location of 18S-5.8S-26S rDNA and a C genome specific DNA sequence in the genus *Avena*. *Genome* **39**, 535-542.

Loidl, J. (1990). The initiation of meiotic pairing: the cytological view. *Genome* **33**, 759-778.

Lukaszewski, A. J. (1997). The development and meiotic behavior of asymmetrical isochromosomes in wheat. *Genetics* **145**, 1155-1160.

Maguire, M. P. (1983). Homologue pairing and synaptic behavior at zygotene in maize. *Cytologia* **48**, 811-818.

Martínez-Pérez, E., Shaw, P., Reader, S., Aragón-Alcaide, L., Miller, T. and Moore, G. (1999). Homologous chromosome pairing in wheat. *J. Cell Sci.* **112**, 1761-1769.

Moens, P. B., Bernelot-Moens, C. and Spyropoulos, B. (1989). Chromosome core attachment to meiotic nuclear envelope regulates synapsis in *Chloealtis* (Orthoptera). *Genome* **32**, 601-610.

Riera-Lizarazu, O., Rines, H. W. and Phillips, R. L. (1996). Cytological and molecular characterization of oat × maize partial hybrids. *Theor. Appl. Genet.* **93**, 123-135.

Roeder, S. G. (1997). Meiotic chromosomes: it takes two to tango. *GenesDev.* **11**, 2600-2621.

Scherthan, H., Bahler, J. and Kohli, J. (1994). Dynamics of chromosome organization and pairing during meiotic prophase in fission yeast. *J. Cell Biol.* **127**, 273-285.

Scherthan, H., Weich, S., Schwegler, H., Heyting, C., Harle, M. and Cremer, T. (1996). Centromere and telomere movements during early meiotic prophase of mouse and man are associated with the onset of chromosome pairing. *J. Cell Biol.* **134**, 1109-1125.

Scherthan, H., Eils, R., Trelles-Sticken, E., Dietzel, S., Cremer, T., Walt, H. and Jauch, A. (1998). Aspects of three-dimensional chromosome reorganization during the onset of human male meiotic prophase. *J. Cell Sci.* **111**, 2337-2351.

Schwarzacher, T. (1997). Three stages of meiotic homologous chromosome pairing in wheat: cognition, alignment and synapsis. *Sex. Plant Reprod.* **10**, 324-331.

Trelles-Sticken, E., Loidl, J. and Scherthan, H. (1999). Bouquet formation in budding yeast: initiation of recombination is not required for meiotic telomere clustering. *J. Cell Sci.* **112**, 651-658.

Von Wettstein, D., Rasmussen, S. W. and Holm, P. B. (1984). The synaptonemal complex in genetic segregation. *Annu. Rev. Genet.* **18**, 331-314.

Weiner, B. A. and Kleckner, N. (1994). Chromosome pairing via multiple interstitial interactions before and during meiosis in yeast. *Cell* **77**, 977-991.

Zickler, D. and Kleckner, N. (1998). The leptotene-zygotene transition of meiosis. *Annu. Rev. Genet.* **32**, 619-697.